25. Lieberman, D. E. Sphenoid shortening and the evolution of modern human cranial shape. *Nature* **393,** 158–162 (1998).
26. Lieberman, D. E., Ross, C. F. & Ravosa, M. J. The primate cranial base: ontogeny, function, and integration. *Yb. Phys. Anthropol.* **43,** 117–169 (2000).
27. Lieberman, D. E. & McCarthy, R. C. The ontogeny of cranial base angulation in humans and chimpanzees and its implications for reconstructing pharyngeal dimensions. *J. Hum. Evol.* **36,** 487–517 (1999).
28. Tattersall, I. & Schwartz, J. H. Morphology, paleoanthropology and Neanderthals. *New Anat.* **253,** 113–117 (1998).
29. Ubelaker, D. H. *Human Skeletal Remains. Excavation, Analysis, Interpretation* (Chicago Univ. Press, Chicago, 1978).
30. Zollikofer, C. P. E. & Ponce de León, M. S. Tools for rapid prototyping in the biosciences. *IEEE Comp. Graph. Appl.* **15,** 48–55 (1995).

Supplementary information is available on *Nature's* World-Wide Web site (http://www.nature.com) or as paper copy from the London editorial office of *Nature.*

Acknowledgements

We are grateful to R. D. Martin and P. Stucki for support of our research. C. B. Stringer's continuous help and advice is gratefully acknowledged. We thank C. Howell, J.-J. Jaeger, D. Lieberman, J. Schwartz and C. Pryce for valuable comments on an earlier version of this paper. We appreciate the help of the following curators in providing access to fossil specimens: J.-J. Cleyet-Merle, J.-M. Cordy, V. Kharitonov, M. Marinot, F. Menghin, R. Orban, I. Pap, Y. Rak, C. B. Stringer, B. Vandermeersch. We also thank the radiologists, physicists and technicians engaged in fossil computer tomography scanning: E. Berenyi, G. Bijl, P. Dondelinger, V. Dousset, W. Fuchs, S. Louryan, V. Makarenko, U. Shreter, N. Strickland and C. L. Zollikofer. This work was supported by the Swiss National Science Foundation and a habilitation grant of the Canton of Zurich.

Correspondence and requests for materials should be addressed to C.Z. (e-mail: zolli@ifi.unizh.ch).

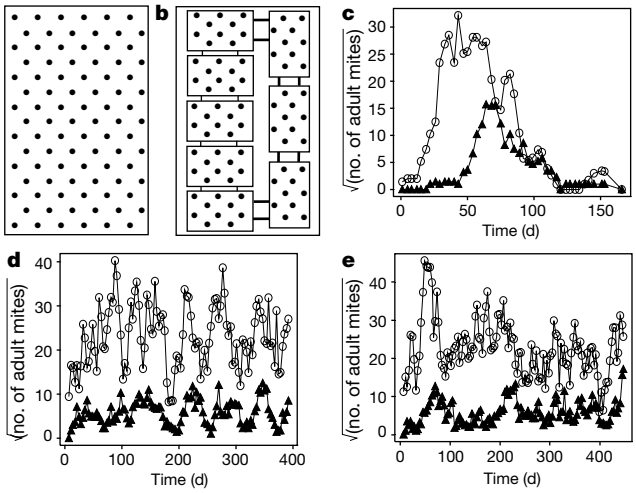

Figure 1 Experimental layouts and results. **a**, The single-island system consisted of a Styrofoam sheet with 90 embedded plants (filled circles) floating in a shallow tray of water. **b**, The metapopulation subdivided the sheet into 8 islands (10 plants per island) connected by cork bridges, with the space for 10 plants being lost. Replicate systems were housed simultaneously in the same environmental chamber, and given identical initial inoculations of mites. **c**, Fluctuations in total density of prey (open circles) and predatory (filled triangles) mites in the single-island experiment. **d**, **e**, Fluctuations in total density of prey (open circles) and predatory (filled triangles) miles in the two replicates of the metapopulation experiment.

Habitat structure and population persistence in an experimental community

Stephen P. Ellner*, Edward McCauley†, Bruce E. Kendall‡, Cheryl J. Briggs§, Parveiz R. Hosseini‖, Simon N. Wood¶, Arne Janssen#, Maurice W. Sabelis#, Peter Turchin☆, Roger M. Nisbet‖ & William W. Murdoch‖

* *Department of Ecology and Evolutionary Biology, Cornell University, Ithaca, New York 14853-2701, USA*
† *Ecology Division, Department of Biological Sciences, University of Calgary, Calgary T2N 1N4, Canada*
‡ *Donald Bren School of Environmental Science and Management; and*
‖ *Department of Ecology, Evolution and Marine Biology, University of California, Santa Barbara, California 93106, USA*
§ *Department of Integrative Biology, University of California, Berkeley, California 94720, USA*
¶ *School of Mathematical and Computation Sciences, University of St Andrews, Fife, Scotland KY16 9SS, UK*
# *Institute for Biodiversity and Ecosystem Dynamics, PO Box 94084, 1090 GB Amsterdam, The Netherlands*
☆ *Department of Ecology and Evolutionary Biology, University of Connecticut, Storrs, Connecticut 06269, USA*

Understanding spatial population dynamics is fundamental for many questions in ecology and conservation[1–4]. Many theoretical mechanisms have been proposed whereby spatial structure can promote population persistence, in particular for exploiter–victim systems (host–parasite/pathogen, predator–prey) whose interactions are inherently oscillatory and therefore prone to extinction of local populations[5–11]. Experiments have confirmed that spatial structure can extend persistence[11–16], but it has rarely been possible to identify the specific mechanisms involved. Here we use a model-based approach to identify the effects of spatial population processes in experimental systems of bean plants

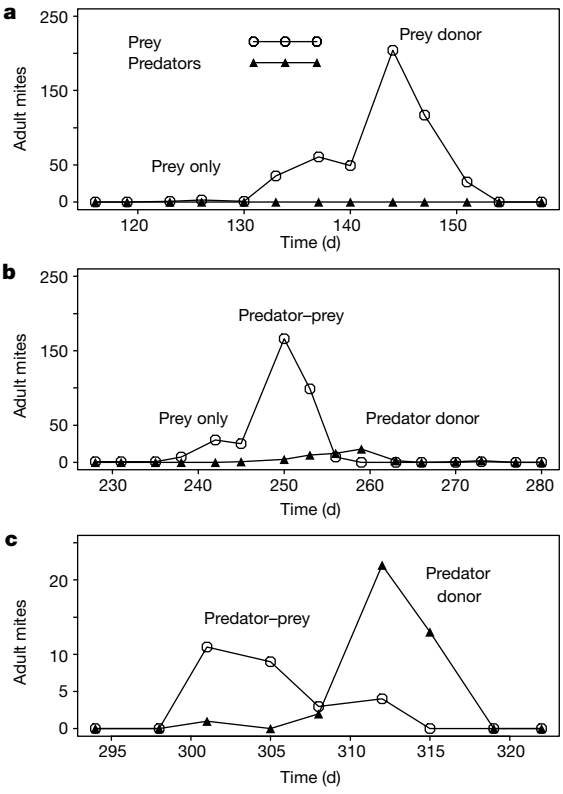

Figure 2 Examples of mite population dynamics on a single plant, from run B of the metapopulation experiment. **a**, A prey outbreak (plant 1, island 5) that was not discovered by predators. The three successively larger peaks in the prey density (days 126, 137 and 144) are the original colonizers, their offspring (counted when they become adults at age ~10 d), and offspring of the offspring. The rapid collapse of the outbreak is primarily due to emigration after exhaustion of the resource. **b**, A prey outbreak (plant 1, island 2) colonized by predators after several on-plant prey generations. Predators arrived too late to prevent growth of the prey population, and the outbreak terminated through exhaustion of the resource and prey emigration. **c**, A prey outbreak (plant 8, island 2) colonized by predators when prey densities were still low. The outbreak terminated through predators consuming all prey and then emigrating.

(*Phaseolus lunatus*), herbivorous mites (*Tetranychus urticae*) and predatory mites (*Phytoseiulus persimilis*). On isolated plants, and in a spatially undivided experimental system of 90 plants, prey and predator populations collapsed; however, introducing habitat structure allowed long-term persistence. Using mechanistic models, we determine that spatial population structure did not contribute to persistence, and spatially explicit models are not needed. Rather, habitat structure reduced the success of predators at locating prey outbreaks, allowing between-plant asynchrony of local population cycles due to random colonization events.

Plants (*P. lunatus*) were grown in individual pots in arrays that were initially free of mites[15] (Fig. 1). Experiments began by placing individual prey mites (*T. urticae*) onto several plants, followed by predatory mites (*P. persimilis*) on the same plants. Mite populations on an individual plant collapse either through the prey exhausting the resource or by predators colonizing the plant, consuming all prey and then starving or emigrating[17] (Fig. 2). The individual plant dynamics did not differ between the single-island (unstructured habitat) and metapopulation (subdivided habitat) systems (Fig. 1a, b), therefore the differing system dynamics must result from effects of habitat structure. The factors are present in the metapopulation system for two distinct but non-exclusive stabilizing mechanisms.

The first mechanism is that spatial subdivision produces differing dispersal scales in predators and prey. In the single-island system, both species dispersed throughout the system, but in the metapopulation system only predators dispersed throughout the system while prey mainly colonized plants on the same or nearby islands[18]. Such differences in dispersal can create spatial patterns where different locations act as source habitat for prey and predators, and total densities are stabilized[19,20]. We tested for such clumped distributions using Moran's I, and found significant ($P < 0.05$) spatial correlation ($I > 0$) among plants on the same island for both mite species on most census dates (85 and 81% for prey; 93 and 92% for predators, in the two metapopulation experiments). The second mechanism is that spatial subdivision reduces the discovery rate of prey outbreaks by predators. Nearly 90% of prey outbreaks were attacked by predators in the single-island experiments, but only 68 and 78% in the two metapopulation experiments[18]. This mechanism has two components, neither involving spatial pattern: reduced average predator success, and the resulting between-plant asynchrony, meaning that not all plants are simultaneously exploited by prey and not all prey outbreaks are simultaneously discovered and extinguished. Hence a non-spatial model for total numbers of plants occupied by each species can describe the system[21].

To determine which mechanism accounts for the observed dynamics, we developed and tested models that allowed us to simulate experiments that would be infeasible in the actual systems. The models consist of colonization probabilities, and nonlinear stage-structure models for the predator–prey–plant interactions occurring on the plant. We assigned parameters to the on-plant interaction models (Box 1) using independent data[22,23]; these were identical for the metapopulation and single-island systems. The equations for colonization probabilities (Box 2) give each plant's daily chance of colonization as a function of the abundance and

Box 1

Structured population models for mite dynamics on a plant

We combined a stochastic description of plant colonizations (Box 2) with a deterministic growth model for mite populations on occupied plants. The stochasticity of individual mites colonizing suitable plants is essential for generating between-plant asynchrony in the model, but the on-plant dynamics involve many individuals and can be modelled deterministically[17,23].

We used nonlinear, stage-structured[26] matrix models[27] with a 1-d time step for the mite populations on each occupied plant. We classified mites by life stage and assigned stage-specific vital rates (described below) derived from empirical age- and sex-specific vital rates[22,23]. Male adults are much smaller than female adults in both species; we gave male adults the same feeding and survival rates as juvenile females (who are similar in size), and assumed a fixed male : female ratio in all stages (1 : 4 in predators; 1 : 3 in prey) rather than explicitly tracking males.

Because pre-adult prey require much less food and rarely experience food shortages, we assumed predation to be the only cause of pre-adult prey mortality. It is a reasonable approximation for prey that daily fecundity is 9 d^{-1} at maturation, and egg production (survival to age × fecundity at age a) subsequently declines by 10% d^{-1}. We therefore modelled adult prey as having a constant fecundity at 9 d^{-1}, and 10% d^{-1} mortality in the absence of predators. Similarly, adult predators were assumed to have constant fecundity (3.2 d^{-1}) and mortality rates (0.04 d^{-1}) when prey are not limiting.

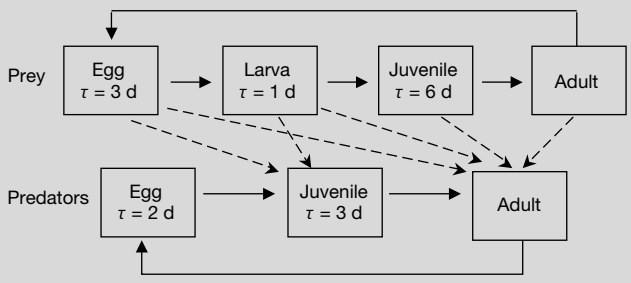

Box 1 Figure

Life stages of prey and predatory mites in the model. Solid arrows indicate survival and fecundity, dashed arrows indicate predation (other mortality losses are omitted for clarity). We assumed constant durations τ for pre-adult stages[22]. Adult stages have indefinite duration, with a constant background mortality rate (0.1 d^{-1} for prey; 0.04 d^{-1} for predators). The resulting models are coupled, nonlinear Leslie matrices of sizes 11 × 11 and 6 × 6 for prey and predators, respectively.

Predator development from egg to adult requires the consumption of 15 prey eggs, which we modelled as a requirement of 5 eggs d^{-1}; adult predators require 12 eggs d^{-1}. On the basis of body mass we modelled prey larvae as equivalent to 1 egg, juveniles and adult males as 12/7 eggs, and adult females as 6 eggs[22]. Predators had a strict feeding preference for prey at younger life stages[23,28]. We assumed predator food requirements and preferences were satisfied unless limited by prey abundance on the plant. Predator fecundity scaled down linearly from its maximum value when food requirements are met, to zero when no feeding occurs. This is a good description for the number of female eggs laid (the fraction of male eggs is higher when prey are scarce[29]). Similarly, we assumed predator survival decreased linearly in proportion to unmet food requirements, to a minimum of 0.2 d^{-1} when no feeding occurs; most mortality occurs when food-deprived predators emigrate and search for another plant with prey.

We assumed that adult, female prey mites damage plant leaf area at a constant daily rate per individual. When the area damaged exceeds a threshold, egg laying ceases, adults begin to emigrate at an increasing rate, and juveniles experience increasing mortality and emigrate when they mature. The emigration model was assigned parameters from observations of isolated plants with only prey mites present: twice-weekly counts of adults on the plant, adults recaptured near the plant, and the percentage of damaged leaf area (A.J. and E. van Gool, unpublished data). The start of emigration coincided with the peak in prey density. We therefore set the damage threshold at the estimated average number of mite days between initial colonization and peak density on plants where prey outbreaks went undetected from the single-island and metapopulation experiments.

Box 2

Colonization probability models

The colonization models are regression models for the conditional probability of an available plant being colonized, given the current and recent mite abundances on each plant, and the state of each plant. Plant states are as indicated in Fig. 2: empty; prey only; prey donor (plant is exhausted and prey are emigrating); predator–prey; and predator donor (all prey consumed and predators emigrating). Either of the donor states is followed by the refractory state, ending with replacement by a fresh plant (following the experimental protocol. Small prey outbreaks (number of adults is always ≤10) were not scored as colonization events or prey-only state; we interpret these as mites exploring a plant without settling. However one adult female of each species was sufficient for the predator–prey state, because a few predators arriving early in an outbreak can consume prey before they mature.

We used logistic regression with stepwise and backward variable selection (as in ref. 18) to identify significant 'risk factors' affecting colonization. Plants were classified by distance from the focal plant (single-island: nearest neighbour, the next nearest neighbour, the next, next-nearest neighbour, and non-neighbour; metapopulation: same island, adjacent island, or non-adjacent island; adding within-island distance classes did not improve the final model). The potential risk factors were the mean conspecific densities within each distance class, the decrease in density between current and previous censuses on donor state plants for the species (an indicator of emigration rate), and prey density on the focal plant for predator colonization. We pooled the two metapopulation experiments and did not consider time-lagged densities because mites tend to find new plants quickly or not at all. As an example, the fitted predator colonization probability (between now and the next census) for a prey-only plant in the metapopulation is:

$$\log[P/(1-P)] = -2.7 + 0.074\ (\text{prey density on plant})^{0.5}$$
$$+ 0.024\ (\text{total predator density on same island})$$
$$+ 0.039\ (\text{total predator decrease on same-island predator donor plants})$$
$$+ 0.021\ (\text{total predator decrease on adjacent-island predator donor plants})$$
$$+ 0.011\ (\text{total predator decrease on non-adjacent-island predator donor plants}$$

spatial distribution of predator and prey mites; these were estimated from the modelled experiments and differed between the metapopulation and single-island systems. However, neither mean colonization rates (number of plants colonized each day) nor their patterns of temporal variation were fitted to the data. Rather, they are predicted by the model from the interaction between on-plant dynamics and the equations for colonization probabilities.

The model dynamics match the experimental results. Nearly all model runs of the single-island system exhibit rapid increase of prey and then predators, followed by extinction (Fig. 3a, b). Extinction of both species occurred within 1 yr in over 99% of 1,000 simulation runs. Replicate runs are highly variable because small chance differences in the success of the predators at detecting the initial prey outbreaks have a large effect on the peak densities reached by prey and then predators. Similarly, the single-island experiment (Fig. 1c) persisted longer than typical model runs (Fig. 3a, b) owing to two late prey outbreaks that started at about day 50, but escaped predation until days 65 and 78.

The metapopulation model, although differing only in its equations of colonization probability, showed long-term persistence much more frequently (Table 1 and Fig. 3c, d), corresponding to the experiments (Fig. 1d, e). Measures of temporal averages (Table 1) and patterns of temporal variation (Fig. 4) were close to those for the experiments. The model also produced spatial correlations similar to those in the experiments (within-island I was significantly positive on 63–90% of sample dates (mean = 74%) for prey; 83–97% of sample dates (mean = 89%) for predators, in 25 model runs with both species persisting). These are strong tests because we did not use any of these summary statistics in assigning parameters to the models. However, the model over-predicts slightly the number of plants occupied by prey while under-predicting the prey colonization rate; the coefficients of variation of population fluctuations were low (possibly because the on-plant population

Table 1 Summary statistics for metapopulation experiments and models with and without spatial pattern at different scales

	Experiments (run1, run2)	Metapopulation (spatial model)	Island shuffle	Plant scramble	Global dispersal	Blur plants on island
Prey						
Mean no.	610, 587	696 (613, 782)	695 (612, 786)	688 (601, 778)	650 (562, 740)	260 (112, 420)
CV (%)	55, 68	48 (41, 57)	48 (41, 56)	48 (41, 57)	51 (43, 59)	205 (172, 250)
Plants occupied	7.8, 8.1	8.7 (7.7, 9.6)	8.6 (7.7, 9.6)	8.6 (7.6, 9.6)	8.2 (7.2, 9.2)	4.1 (1.9, 6.4)
Colonization rate (plants d^{-1})	0.83, 0.84	0.61 (0.56, 0.67)	0.61 (0.56, 0.67)	0.61 (0.56, 0.67)	0.60 (0.55, 0.66)	0.43 (0.36, 0.48)
Predators						
Mean no.	42, 47	44 (34, 54)	44 (34, 54)	45 (36, 56)	47 (36, 58)	61 (37, 83)
CV (%)	87, 104	74 (60, 89)	74 (61, 88)	73 (60, 88)	74 (60, 88)	223 (184, 275)
Plants occupied	7.0, 7.8	6.6 (5.7, 7.7)	6.6 (5.8, 7.6)	6.8 (5.8, 7.8)	6.9 (6.0, 7.9)	9.1 (6.8, 10.8)
Colonization rate (plants d^{-1})	0.52, 0.59	0.48 (0.42, 0.54)	0.48 (0.42, 0.54)	0.49 (0.43, 0.55)	0.50 (0.44, 0.56)	0.83 (0.63, 1.09)
Persistence						
Prey (% of runs)	yes, yes	100	100	100	100	1.8
Both species (% of runs)	yes, yes	81	79	81	80	0.08

Values for the models are mean values (5th and 95th percentiles in parentheses) from 1,000 runs (50,000 for plant blur), averaging over runs in which both species persisted for 400 d. Model runs in which one or both species go extinct are not comparable to the experiments, in which both species persisted. Data from the first 30 d of the experiments and simulations were omitted to eliminate transients. Plants were scored as occupied by prey (for model output and experimental data) only when ten or more adults were present, to eliminate the frequent counts of a few stray prey in the experimental systems not associated with a prey outbreak on a plant. CV, coefficient of variation.

models are deterministic); and the time lags between changes in prey abundance and the resulting changes in predator abundance and colonization rate were under-predicted by roughly 3 d.

The differing temporal autocorrelations between the two metapopulation experiments[15] (Fig. 4c–f) are also consistent with the model. The first wave of predator colonizations was much smaller in the second experiment (Fig. 1e) than in the first (Fig. 1d), resulting in higher prey densities and a deeper subsequent crash by both species. This pattern also occurred in about 15% of model runs where initial predator growth was restricted.

We determined which aspects of spatial dynamics were responsible for persistence in the metapopulation by systematically eliminating different aspects of spatial pattern in simulations. Under the first mechanism, eliminating spatial pattern at the island and metapopulation levels should produce dynamics similar to those observed in the single-island system. Under the second mechanism, reducing local between-plant asynchrony should have this effect. In 'island shuffling' simulations, the sequence of islands in the ring (Fig. 1b) was randomly shuffled each day, but plants remained on their home island. This preserves within-island correlation but eliminates pattern at the metapopulation level. In 'plant scrambling' simulations the location of all plants was randomized each day, and in 'global dispersal' simulations, all colonization probabilities were calculated from system-wide average densities rather than local densities. These simulations eliminate spatial pattern at the island and metapopulation level, but retain between-plant asynchrony. In 'plant blurring' simulations, the age-specific mite densities on each plant were replaced daily by the average density over all plants on the same island. This eliminates within-island asynchrony but preserves pattern at the metapopulation level.

Island shuffling, plant scrambling and global dispersal had only small effects on the dynamics (Table 1, Figs 3 and 4). Plant scrambling eliminated within-island autocorrelations because each island is reassembled daily at random, but autocorrelations of total densities were unaffected (Fig. 4). In contrast, plant blurring produced extinction similar to the single-island experiment (Fig. 3i, j) with predators finding all prey outbreaks because of the rapid within-island dispersal. The reduced system size with blurring (8 islands versus 80 plants) still allows enough asynchrony for prey persistence in the absence of predators (81% of 1,000 runs).

These results indicate that the first stabilizing mechanism is not responsible for long-term persistence in the metapopulation

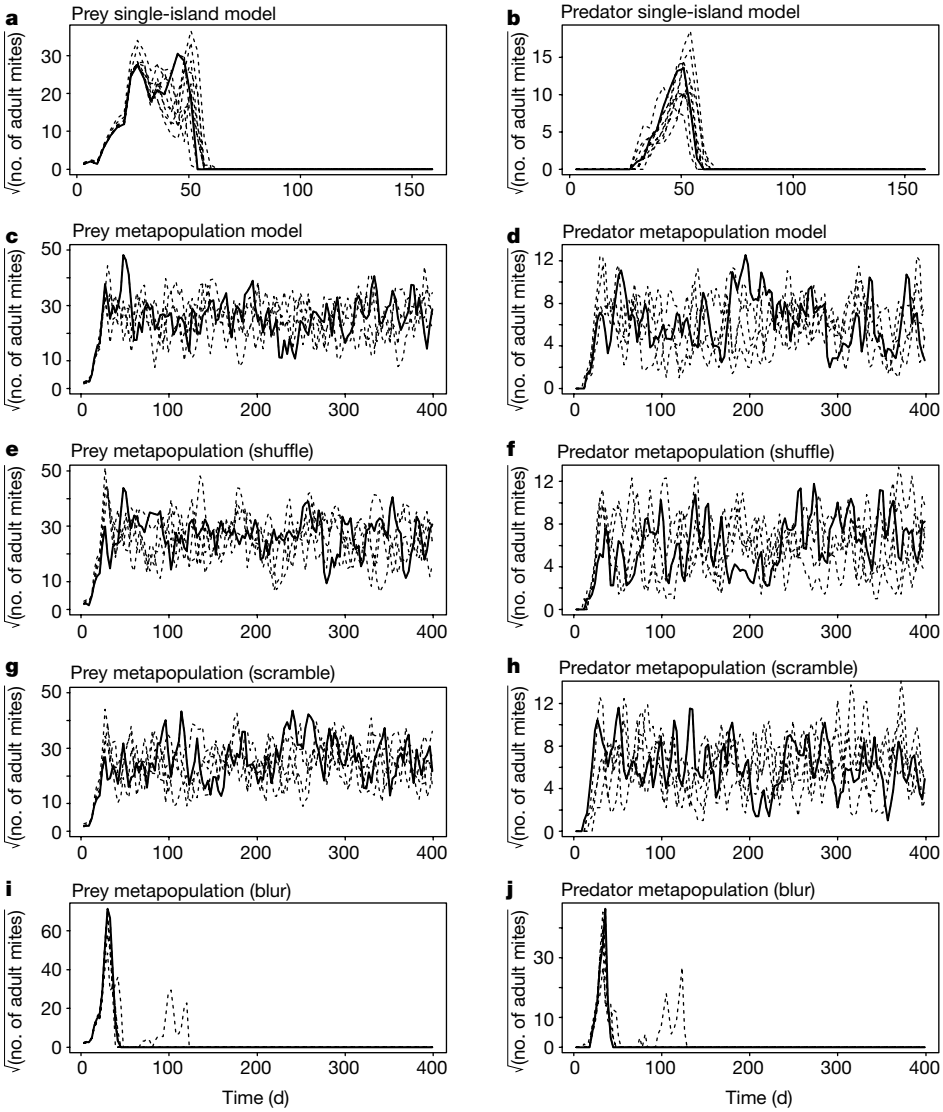

Figure 3 Total prey and predator mite densities in consecutive replicate runs of the simulation models. The first run is plotted as a solid line, the rest as dashed lines. **a**, **b**, Single-island model. **c**, **d**, Metapopulation model. **e**, **f**, Metapopulation model with island shuffling. **g**, **h**, Metapopulation model with plant scrambling. **i**, **j**, Metapopulation model with plant blurring; note the change in scale. For panels **c**–**h** we show only runs in which both species persist to day 400, which is a typical result (Table 1).

system, and are consistent with the second mechanism. If the second mechanism caused persistence, decreasing the predators' success at detecting prey outbreaks in the single-island should result in persistence. We tested this prediction in the single-island model by reducing daily probability of predators finding each prey-only plant by a factor P ($0.05 < P < 1$). The probability of both species persisting for 360 d was highest when about 25% of prey outbreaks escape detection (88% of 1,000 runs at $P = 0.1$), which is similar to the actual values in the metapopulation experiments (22 and 32%). Conversely, the metapopulation model persisted less often when predator colonization probabilities were increased.

Thus, the dynamics of the systems results mainly from the average probability that prey mites find unoccupied plants, the average probability that predators find a prey outbreak, and the stochasticity of individual colonization events. The systems can be modelled successfully without regard to the spatial location of plants, as in classical models for metapopulation[24] and host–parasitoid dynamics[5]. A preliminary 'metapopulation swapping' experiment is consistent with this conclusion (Supplementary Information).

Comparison of alternative mechanistic models is a powerful approach for testing hypotheses regarding processes responsible for patterns in ecological dynamics. By comparing models with different assumptions about the effects of habitat subdivision, we have shown that the one essential process allowing persistence of the metapopulation was one of the earliest and simplest hypotheses about spatial dynamics: isolation by distance[9,21,24,25]. Habitat subdivision increased the effective distance between plants from the viewpoint of the predators, giving prey a moving refuge from their enemies. □

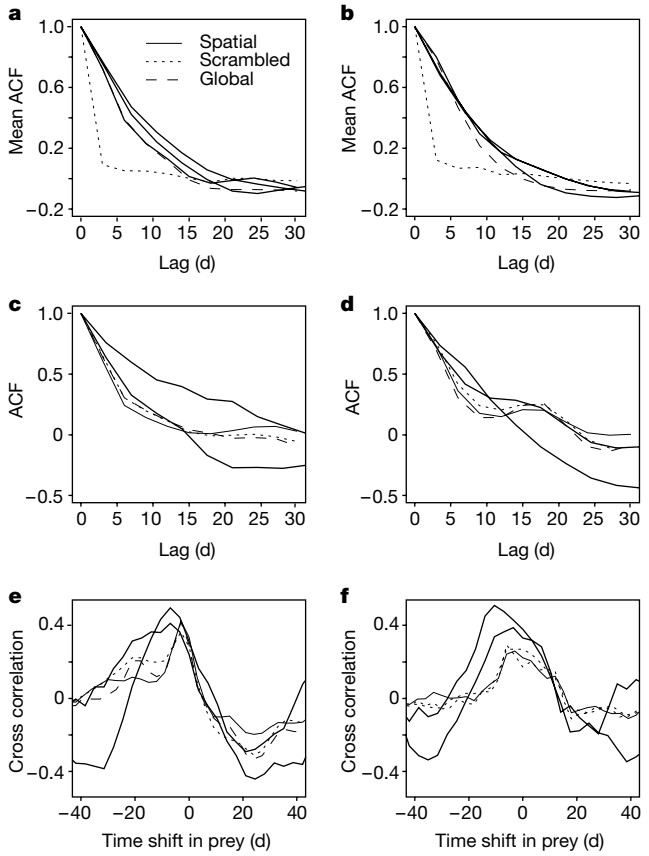

Figure 4 Summary measures of temporal patterns in model output and experimental results. In all panels the thick solid curves are the two metapopulation experiments, the thin solid curve is the metapopulation model, the dotted curve is the metapopulation model with plant scrambling (plant locations randomized each day), and the dashed curve is the model with global dispersal among plants irrespective of location. Curves for model output are the average over 10 replicate runs in which both species persist for 400 d. Correlations were calculated on square-root-transformed population counts; counts of colonization events were not transformed. **a**, **b**, Average across islands of the autocorrelation function (ACF) for the time series of total density on an island (8 series each for prey (**a**) and predator (**b**)). **c**, **d**, Autocorrelation function of the system-wide total prey (**c**) and predator (**d**) densities. **e**, Cross correlation between system-wide total prey density at time $(t + L)$ and total predator density at time t, as a function of the time shift L. **f**, Cross correlation between total prey density at time $(t + L)$ and the predator colonization rate (plants d^{-1}) at time t, as a function of the time shift L. Plant scrambling has large effects at the island level (**a** and **b**) but has only small effects at the system-wide level (**c**–**f**).

Methods

Experimental design

We counted adult female mites on each plant twice a week. After all mites had left a plant (three consecutive samples without prey or four without predators, whichever occurred last), it was replaced with a 1-week-old plant pruned to two leaves. We regularly pruned plants and replaced uncolonized plants with 1-week-old plants, to standardize conditions and eliminate direct connections among plants. Mites dispersed only by walking from one plant to another. Because the bridges between islands in the metapopulation were positioned below the island rim, mites often missed these connections, reducing inter-island movements. See ref. 15 for further experimental details. Initial prey inoculations in the models were identical to the experiments, matching the day, plant and number of individuals added. Predator inoculations in the models corresponded in the same way to successful predator inoculations in the experiments (those where the founding predator reproduced and established a local population).

Received 27 March; accepted 20 June 2001.

1. Tilman, D. & Kareiva, P. (eds) *Spatial Ecology: the Role of Space in Population Dynamics and Interspecific Interactions* (Princeton Univ. Press, Princeton, 1997).
2. Dieckmann, U., Law, R. & Metz, J. A. J. (eds) *The Geometry of Ecological Interactions: Simplifying Spatial Complexity* (Cambridge Univ. Press, Cambridge, 2000).
3. Hanski, I. A. & Gilpin, M. E. (eds) *Metapopulation Biology: Ecology, Genetics, and Evolution* (Academic, San Diego, 1997).
4. Levin, S. A., Grenfell, B., Hastings, A. & Perelson, A. S. Mathematical and computational challenges in population biology and ecosystems science. *Science* **275,** 334–343 (1997).
5. May, R. M. Host–parasitoid systems in patchy environments: a phenomenological model. *J. Anim. Ecol.* **47,** 833–843 (1978).
6. Sabelis, M. W. & Diekmann, O. Overall population stability despite local extinction: the stabilizing effect of prey dispersal from predator-invaded patches. *Theor. Popul. Biol.* **34,** 169–176 (1988).
7. Hassell, M. P. & May, R. M. Spatial heterogeneity and the dynamics of parasitoid–host systems. *Ann. Zool. Fenn.* **25,** 55–61 (1988).
8. Hassell, M. P., Comins, H. N. & May, R. M. Spatial structure and chaos in insect population dynamics. *Nature* **353,** 255–258 (1991).
9. de Roos, A. M., McCauley, E. & Wilson, W. Mobility versus density limited predator–prey dynamics on different spatial scales. *Proc. R. Soc. Lond. B* **246,** 117–122 (1991).
10. Sabelis, M. W., Diekmann, O. & Jansen, V. A. A. Metapopulation persistence despite local extinction—predator–prey patch models of the Lotka-Volterra type. *Biol. J. Linn. Soc.* **42,** 267–283 (1991).
11. Murdoch, W. W. Population regulation in theory and practice. *Ecology* **75,** 271–287 (1994).
12. Huffaker, C. B., Shea, K. P. & Herman, S. G. Experimental studies on predation: complex dispersion and levels of food in an acarine predator–prey interaction. *Hilgardia* **34,** 305–330 (1963).
13. van de Klashorst, G., Readshaw, G. L., Sabelis, M. W. & Lingeman, R. A demonstration of asynchronous local cycles in an acarine predator–prey system. *Exp. Appl. Acarol.* **14,** 185–199 (1992).
14. Holyoak, M. & Lawler, S. P. Persistence of an extinction prone predator–prey interaction through metapopulation dynamics. *Ecology* **77,** 1867–1879 (1996).
15. Janssen, A., van Gool, E., Lingeman, R., Jacas, J. & van de Klashorst, G. Metapopulation dynamics of a persisting predator–prey system in the laboratory: time-series analysis. *Exp. Appl. Acarol.* **21,** 415–430 (1997).
16. Holyoak, M. Habitat patch arrangement and metapopulation persistence of predators and prey. *Am. Nat.* **156,** 378–389 (2000).
17. Pels, B. & Sabelis, M. W. Local dynamics, overexploitation and predator dispersal in an acarine predator–prey system. *Oikos* **86,** 573–583 (1999).
18. McCauley, E. *et al.* Inferring colonization processes from population dynamics in spatially structured predator–prey systems. *Ecology* **81,** 3350–3361 (2000).
19. McCauley, E., de Roos, A. M. & Wilson, W. Dynamics of age- and spatially-structured predator–prey interactions: individual based models and population level formulations. *Am. Nat.* **142,** 412–442 (1993).
20. de Roos, A. M., McCauley, E. & Wilson, W. Pattern formation and the spatial scale of interactions between predators and their prey. *Theor. Popul. Biol.* **53,** 108–130 (1998).
21. Nisbet, R. M. & Gurney, W. S. C. *Modelling Fluctuating Populations* Ch. 10 (Wiley, New York, 1982).
22. Helle, W. & Sabelis, M. W. (eds) *Spider Mites, their Biology, Natural Enemies, and Control* (Elsevier, Amsterdam, 1985).
23. Sabelis, M. W. & van der Meer, J. in *Dynamics of Physiologically Structured Populations* (eds Metz, J. A. J. & Diekmann, O.) 322–344 (Springer, New York, 1986).
24. Hastings, A. Spatial heterogeneity and stability of predator–prey systems. *Theor. Popul. Biol.* **12,** 37–48 (1977).
25. Wright, S. Isolation by distance. *Genetics* **28,** 114–138 (1943).
26. Gurney, W. S. C., Nisbet, R. M. & Lawton, J. H. The systematic formulation of tractable single-species population models incorporating age structure. *J. Anim. Ecol.* **52,** 479–495 (1983).

27. Caswell, H. *Matrix Population Models: Construction, Analysis, and Interpretation* (Sinauer Associates, Sunderland, Massachusetts, 2001).
28. Sabelis, M. W. How to analyze prey preference when prey density varies? A new method to discriminate between effects of gut fullness and prey type composition. *Oecologia* **82,** 289–298 (1990).
29. Sabelis, M. W. & Nagelkerke, C. J. Sex allocation strategies of pseudoarrhenotokous phytoseiid mites. *Neth. J. Zool.* **37,** 117–136 (1987).

Supplementary information is available at *Nature*'s World-Wide Web site (http://www.nature.com) or as paper copy from the London editorial office of *Nature*.

Acknowledgements

We thank E. van Gool for assistance with the experiments. This work was undertaken as part of the Working Group on Complex Population Dynamics at the National Center for Ecological Analysis and Synthesis, a centre funded by the US National Science Foundation, University of California–Santa Barbara, and the State of California. A.J. and M.W.S. carried out experiments; E.M., B.E.K., C.J.B. and S.N.W. conceived and fitted colonization models; S.P.E., S.N.W., P.R.H., A.J., P.T., R.M.N. and W.W.N. conceived and fitted structured population models; S.P.E., P.R.H., S.N.W. and C.J.B. implemented the models; S.P.E., E.M. and B.E.K. carried out comparisons of models with data; and S.P.E., E.M., A.J., M.W.S. and P.R.H. prepared the original manuscript.

Correspondence and requests for materials should be addressed to S.P.E. (e-mail: spe2@cornell.edu).

The end of world population growth

Wolfgang Lutz*, Warren Sanderson*† & Sergei Scherbov‡

* *International Institute for Applied Systems Analysis, Schlossplatz 1, A-2361 Laxenburg, Austria*
† *Departments of Economics and History, State University of New York at Stony Brook, New York 11794-4384, USA*
‡ *University of Groningen, PO Box 800, NL-9700 AV Groningen, The Netherlands*

There has been enormous concern about the consequences of human population growth for the environment and for social and economic development. But this growth is likely to come to an end in the foreseeable future. Improving on earlier methods of probabilistic forecasting[1], here we show that there is around an 85 per cent chance that the world's population will stop growing before the end of the century. There is a 60 per cent probability that the world's population will not exceed 10 billion people before 2100, and around a 15 per cent probability that the world's population at the end of the century will be lower than it is today. For different regions, the date and size of the peak population will vary considerably.

Figure 1 shows the probability that the world population size would reach a peak at or before any given year. It indicates that there is around a 20 per cent chance that the peak population would be reached by 2050, around a 55 per cent chance that it would be reached by 2075, and around an 85 per cent chance that it would be reached by the end of the century.

There is around a 75 per cent chance that the peak population of the European portion of the former USSR has already been reached in 2000, an 88 per cent probability that it will be reached by 2025, and over a 95 per cent chance by the end of the century. For the China region, the probability of reaching a peak within the next two decades is still low owing to its relatively young age structure. By 2040 the probability becomes greater than half. In sub-Saharan Africa, despite the prevalence of HIV, there is a low probability of peaking before the middle of the century. The probability reaches 25 per cent by 2070, 50 per cent by 2085, and almost 75 per cent by 2100, owing to assumed reductions in fertility.

Figure 2 shows the distribution of simulated world population sizes over time. The median value of our projections reaches a peak around 2070 at 9.0 billion people and then slowly decreases. In 2100,

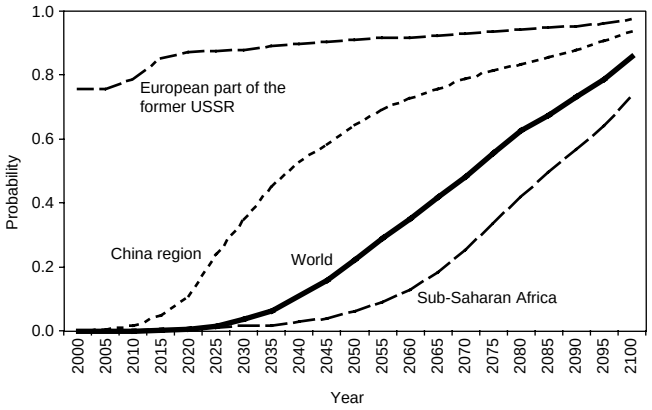

Figure 1 Forecasted probability that population will start to decline at or before the indicated date.

the median value of our projections is 8.4 billion people with the 80 per cent prediction interval bounded by 5.6 and 12.1 billion. The medium scenario of the most recent United Nations long-range projection[2] is inserted in Fig. 2 as a white line. It is almost identical to our median until the middle of the century, but is higher thereafter owing to the United Nations assumption of universal replacement-level fertility, that is two surviving children per woman.

Table 1 shows the median population sizes and associated 80 per cent prediction intervals for the world and its 13 regions, indicating major regional differences in the paths of population growth. While over the next two decades the medians are already declining in eastern Europe and the European portion of the former Soviet Union, the populations of north Africa and sub-Saharan Africa are likely to double, even when we take into account the uncertainty about future HIV trends.

The China region and the South Asia region, which have approximately the same population size in 2000, are likely to follow very different trends. Owing to an earlier fertility decline, the China region is likely to have around 700 million fewer people than the South Asia region by the middle of the century. This absolute difference in population size is likely to be maintained over the entire second half of the century and illustrates the strong impact of the timing of fertility decline on eventual population size[3].

Our findings concerning the timing of the end of world population growth are robust to plausible changes in parameter assumptions. A detailed sensitivity analysis is provided as Supplementary Information. The forecasts of the World Bank, the US Census Bureau, and the medium variant of the United Nations[2,4,5] are based on independent assumptions; the median trajectory of our world forecasts is almost identical to these up until 2045. Of these three forecasts, only the UN long-range projections provide scenarios of the world's population to the end of the century. If we define the end of population growth slightly less literally, and take it to correspond with annual population growth of one-tenth of one per cent or less, the United Nations medium projection also shows the end of population growth during the second half of the century. Their medium scenario predicts that world population growth will first fall below one-tenth of one per cent at around 2075.

A stabilized or shrinking population will be a much older population. At the global level the proportion above age 60 is likely to increase from its current level of 10 per cent to around 22 per cent in 2050. This is higher than it is in western Europe today. By the end of the century it will increase to around 34 per cent, and extensive population ageing will occur in all world regions. The most extreme levels will be reached in the Pacific OECD (mostly Japan), where half of the population is likely to be age 60 and above by the end of the century, with the 80 per cent uncertainty interval